

Catalysis Science & Technology

Accepted Manuscript

This article can be cited before page numbers have been issued, to do this please use: Q. Zhou, D. Li, B. Ding, A. Zheng, R. Zhang, Y. Yao, X. Gong and Z. Hou, *Catal. Sci. Technol.*, 2020, DOI: 10.1039/D0CY01401J.



This is an Accepted Manuscript, which has been through the Royal Society of Chemistry peer review process and has been accepted for publication.

Accepted Manuscripts are published online shortly after acceptance, before technical editing, formatting and proof reading. Using this free service, authors can make their results available to the community, in citable form, before we publish the edited article. We will replace this Accepted Manuscript with the edited and formatted Advance Article as soon as it is available.

You can find more information about Accepted Manuscripts in the [Information for Authors](#).

Please note that technical editing may introduce minor changes to the text and/or graphics, which may alter content. The journal's standard [Terms & Conditions](#) and the [Ethical guidelines](#) still apply. In no event shall the Royal Society of Chemistry be held responsible for any errors or omissions in this Accepted Manuscript or any consequences arising from the use of any information it contains.

Ionic Liquid-Stabilized Vanadium Oxo-clusters Catalyzing Alkane Oxidation by Regulating Oligovanadates

View Article Online
DOI: 10.1039/C0CY01401J

Qingqing Zhou^a, Ran Zhang^b, Difan Li^a, Bingjie Ding^a, Anna Zheng^a, Yefeng Yao^{*b},
Xueqing Gong^a and Zhenshan Hou^{*a}

^aKey Laboratory for Advanced Materials, Research Institute of Industrial Catalysis, East China University of Science and Technology, Shanghai 200237, China

^bPhysics Department and Shanghai Key Laboratory of Magnetic Resonance, East China Normal University, Shanghai 200062, China.

* Corresponding author. E-mail address: houzhenshan@ecust.edu.cn (Z. Hou).

Abstract: The alkane oxidation under mild conditions occupies an important position in the chemical industry. Herewith, we have designed a novel class of ionic liquid ([TBA][Pic])-stabilized vanadium oxo-clusters (TBA=tetrabutylammonium; Pic=picolinate ions), in which the molar ratio of the IL to V atoms can be tuned facilely to obtain V-OC@IL-0.5, V-OC@IL-1 and V-OC@IL-2, respectively. The as-synthesized vanadium oxo-clusters have been characterized by element analysis, FT-IR, Uv-vis, XRD, TGA, EPR, NMR and MS. These vanadium oxo-clusters were catalytically active for the catalyzing oxidation of cyclohexane with H₂O₂ as an oxidant. Especially, the oxo-cluster V-OC@IL-1 (where IL/V is 1.0) can provide approximately 30% total yield of KA oil (cyclohexanol and cyclohexanone) without adding any co-catalyst at 50 °C within 1.0 h. Moreover, the present vanadium oxo-cluster was recyclable owing to the modification of IL and it also can be extended for the oxidation of the sp² hybrid aromatic ring. The further characterization results demonstrated that the oligovanadate anions were strongly dependent on the molar ratio of the IL to V atoms. The vanadium oxo-clusters with the appropriate molar ratio of IL/V could exist in the form of trimer and dimer due to the presence of TBA cation and the coordination of picolinate. Notably, the oligovanadate anions are highly active species for the C–H oxidation but the mononuclear vanadate afforded a very poor activity according to the activity assessment and the identification of vanadium species by ⁵¹V NMR spectra and MS spectra. The annihilation reaction of free radicals and EPR characterization suggested that the vanadium oxo-clusters operated via a mechanism of the HO· radical in oxidation reaction.

Keywords: Vanadium, Oxo-cluster, Ionic liquid, Oxidation, Cyclohexane

Introduction

View Article Online
DOI: 10.1039/D0CY01401J

Selective oxidation of hydrocarbons is essential for the production of high-value-added chemicals in current industrial and fine-chemical processes.¹⁻⁴ In particular, Cyclohexane oxidation to cyclohexanone (K) or cyclohexanol (A) (also known as KA oil) is widely recognized and used as one of the fundamental processes in organic chemistry and chemical industry, which can yield further high value-added chemicals, such as polyamide fibers and plastics.⁵⁻⁷ Currently, oxygen, as a cheap and easily available oxidant, is widely utilized for cyclohexane oxidation, which is the most promising oxidant for industrial application. In fact, this reaction has been realized in industry through the autooxidation pathway promoted by cobalt complex.⁵ However, in practice, the conversion of cyclohexane must be kept at a low level of 3–8% in order to achieve an acceptable selectivity > 80% toward the two major commercial products cyclohexanol and cyclohexanone via reducing undesirable by-products. Meanwhile, there are many reports that hydrogen peroxide is used as an oxidant to catalyze the oxidation of cyclohexane. Compared with oxygen, hydrogen peroxide has the advantages that the oxidant is always used under much milder reaction conditions, and can provide a higher yield of KA oil. Hence, in this work we explored the use of hydrogen peroxide as oxidant, and searched for an efficient, selective, environmentally benign and economic approach towards the sustainable development of such an important oxidation process.

In recent years, vanadium-based compounds have shown fast reversible multi-electron redox transformations under rather mild conditions and promising potential for the oxidation of alkanes.⁸⁻¹⁵ Among these important publications, Shul'pin and co-workers have found that pyrazine-2-carboxylic acid (PCA) and analogous compounds (2,3-pyrazinedicarboxylic, picolinic, and dipicolinic acids) can be used as highly active co-catalysts in the vanadate-catalyzed oxidations of alkanes, arenes, alcohols, and other substrates, under mild conditions by peroxides in air.¹⁶ Taking $[\text{VO}_3]^-/\text{PCA}/\text{H}_2\text{O}_2$ system as an example, TBAVO₃ (TBA= tetrabutylammonium) alone showed almost no catalytic activity, while the addition of PCA as an auxiliary greatly improved the catalytic activity of cyclohexane oxidation. It was suggested that the coordination of the carboxylate anion (PCA) to the vanadium is a prerequisite for catalysis.¹⁷ Moreover, the presence of acid is the crucial factor in this process, since in the neutral medium, monovanadate is a dominant species but inactive for catalytic oxidation. The role of the

acid is explained by the formation of oligovanadates in acidic medium, which exhibits much higher catalytic activity compared with the monovanadate. However, these acidic homogeneous catalysts cannot be recycled, causing waste and pollution to the products. Therefore, to develop neutral, catalytically active and easily separable V-based catalysts is highly desirable.

Ionic liquids (ILs), owing to their unique properties like nonvolatility, strong dissolution, low flash point, recyclability and high thermal stability etc., have become promising alternatives to conventional volatile liquid solvents in chemical reaction and separation. Particularly, they are serving as designable media to exhibit a rate acceleration effect on catalytic reactions by modulating coordination, hydrogen bonding and electrostatic interaction etc.¹⁸⁻²⁰ In many circumstances, for easy separation and recyclable utilization, the functionalized ILs have attracted unprecedented attention as “biphasic catalyst” or “immobilized catalyst” for the multiphase reactions and do not require an additional organometallic complex as catalyst. In our previous work, the α -hydroxy carboxylate IL was proved to act as an indispensable agent to stabilize Nb oxo-clusters, in which anions (lactate) formed a layer around the surface of the oxo-cluster, leading to a center of negative charge, and the cations of IL (TBA) existed at the outer layer for charge balance. Besides, the external layer around the nanostructure could prevent aggregation through both steric and electronic protection.²¹⁻²⁵ In particular, the resulting Nb oxo-clusters exhibited an excellent activity for the oxidation of thioethers (TON up to 14754), as well as epoxidation of olefins and allylic alcohols (TON up to 1422) by using only 0.065 mol% of the catalyst (50 ppm).²⁶

The present work concerns a novel IL [TBA][Pic]-induced the aggregates of vanadium species, in which both the picolinate anion and TBA cation play a crucial role in stabilizing oligovanadate species. At the initial stages of this work, we took much effort to synthesize the nano-sized V oxo-cluster by using the functional IL. Surprisingly, it was found that the peroxy-vanadate acid precursor has been transformed into the mixed valence oligomeric vanadates in the presence of the IL. The further results indicated that the oligomeric vanadates existed in the form of the dimer and trimer, and the oligomeric vanadium species favored the oxidation of carbon-hydrogen bonds. Notably, the states of vanadium species can be tuned flexibly by changing the molar ratio of IL and V atoms, which was closely relevant to catalytic activity of

View Article Online
DOI: 10.1039/DOCY01401J

cyclohexane oxidation. This study provides a key role in the peroxy-bond cleavage to give HO· radical species for the oxidation of alkane. It also concerns the perspective of tuning oligomeric states of vanadate anions for such an oxidation reaction. These issues also deserve to be further explored and can open up a new window to the vanadium oxidation catalysis.

View Article Online
DOI: 10.1039/C0CY01401J

Experimental Section

Materials

The commercial vanadium pentoxide (V_2O_5) was obtained from Ailan (Shanghai) Chemical Technology Co., Ltd. Tetrabutylammonium hydroxide (25% aqueous solution) was obtained from Shanghai Lingfeng Chemical Reagent Co., Ltd. 2-picolinic acid (AR) and various substrates were obtained from Sinopharm Chemical Reagent Co., Ltd. (Shanghai, China). Vanadium oxytrichloride was obtained from Bailingwei Technology Co., Ltd. Tetrabutylammonium acetate ([TBA][OAc]) was purchased from Adamas Reagent Co., Ltd. 1-butyl-3-methylimidazolium acetate ([BMIM][OAc]) and 1-butyl-3-methylimidazolium tetrafluoroborate [BMIM][BF₄] were prepared according to the standard procedure.²⁷

Catalyst characterization

The FT-IR spectra were recorded at room temperature on a Nicolet Magna 550 FT-IR spectrometer. The X-ray diffraction (XRD) analysis was performed with D/MAX 2550 VB/PC using CuK α radiation ($\lambda = 1.5406 \text{ \AA}$) operated at 40 kV and 200 mA (scan rate: 6° min^{-1} ; scan area: $5\text{--}75^\circ$). The thermal stability of catalysts was determined by TGA method. A Perkin Elmer Pyris Diamond was used for the TGA measurements. All samples were vacuumed at 60° C for 1 h to remove the solvent molecules before TGA. The samples were heated from 40° C to 800° C (heating rate: $10^\circ \text{ C min}^{-1}$) under the flow of anhydrous air (flow rate: 20 mL min^{-1}). The elemental analysis of C, H, N was performed using an Elementar vario EI III C H N O S elemental analyzer and the ICP-AES analysis of vanadium on a Varian 710 instrument, respectively. The melting point of the IL [TBA][Pic] was recorded with a WRX-2S micro thermal analyzer (Shanghai INESA Physico-Optical Instrument Co.,Ltd.) The mass spectra of catalysts were investigated by MALDI-TOF, with *a*-cyano-4-hydroxycinnamic acid as matrix in H₂O. Electro-Spin Resonance (ESR) spectrum was recorded with a Bruker EMX-8/2.7

at 298 K. Instrument settings: microwave bridge frequency, 9.8 GHz; microwave bridge attenuator, 20 dB; modulation frequency, 100 kHz; modulation amplitude, 5 G; center field, 3500 G. ^1H NMR and ^{13}C NMR spectra were recorded on a Bruker AVANCE 400 MHz instrument (400 MHz ^1H NMR, 100 MHz ^{13}C NMR) using D_2O as solvents and TMS as the reference, respectively. ^{51}V NMR spectra were obtained at room temperature in D_2O on a Varian 700 MHz spectrometer operating at 183.92 MHz. The vanadium chemical shifts are quoted relative to external VOCl_3 in CDCl_3 . The reaction products were analyzed by using Gas chromatography (GC) [a Shimadzu GC-2014 gas chromatograph equipped with the RTX-5MS capillary column ($30\text{ m} \times 0.25\text{ mm} \times 0.25\text{ mm}$)]. The products were also identified by GC-MS [Agilent 6890/5973 GC-MS equipped with the HP-5MS column ($30\text{ m} \times 0.25\text{ mm} \times 0.25\text{ mm}$)].

Preparation of picolinate IL

Picolinate IL ([TBA][Pic]) was prepared by a careful neutralization of 2-picolinic acid with 25% aqueous TBAOH solution (1:1 molar ratio) in water at room temperature. After the solution was stirred for a few hours, followed by drying under vacuum at $60\text{ }^\circ\text{C}$ for 1 h, the IL was obtained as a colorless solid at room temperature, but became a liquid on heating. [TBA][Pic] (m.p.: $37.5\text{ }^\circ\text{C}$), ^1H NMR (400 MHz, D_2O , Me_4Si) δ 8.40 (m, 1H), 7.72 (m, 1H), 7.62 (m, 1H), 7.16 (m, 1H), 3.19 (m, 8H), 1.57 (m, 8H), 1.30 (m, 8H), 0.92 (dt, $J = 8.0\text{ Hz}$, 12H). ^{13}C NMR (100 MHz, D_2O , Me_4Si): δ 172.93, 153.24, 148.29, 137.93, 125.64, 123.62, 57.99, 23.02, 19.06, 12.76. Anal. Calcd for $\text{C}_{19}\text{H}_{41}\text{NO}_3$ ([TBA][Pic]) (333.54): C, 72.5; H, 11.1; N, 7.7. Found: C, 72.4; H, 11.0; N, 7.7.

Preparation of IL-stabilized vanadium oxo-cluster

First, a clear solution was obtained by mixing V_2O_5 (0.091 g, 0.5 mmol) with 30% hydrogen peroxide (1.0 mL) in an ice bath. Then 5.0 mL of aqueous solution containing 1.0 mmol of ionic liquid [TBA][Pic] was added ([TBA][Pic]/V=1.0). After stirred several hours, it was heated to $40\text{ }^\circ\text{C}$ and stirred overnight to evaporate water. Finally, a brown and highly viscous liquid was obtained as V-OC@IL-1. ^1H NMR (400 MHz, D_2O , Me_4Si) δ 8.77-7.62 (m, 4H), 3.19 (m, 8H), 1.56 (m, 8H), 1.30 (m, 8H), 0.92 (dt, $J = 8.0\text{ Hz}$, 12H). ^{13}C NMR (100 MHz, D_2O , Me_4Si): δ 172.93, 153.24, 148.30, 137.95, 125.65, 123.63, 58.00, 23.08, 19.07, 12.77. Found: C, 46.9; H, 7.1; N, 5.9; V, 10.6.

Number of peroxy-bonds: 0.35 per V atom. Similarly, the vanadium oxo-clusters with the different molar ratio of [TBA][Pic] to vanadium were denoted as V-OC@IL-0.5, V-OC@IL-1.5 and V-OC@IL-2, respectively.

V-OC@IL-0.5: ^1H NMR (400 MHz, D_2O , Me_4Si) δ 8.77-7.62 (m, 4H), 3.19 (m, 8H), 1.56 (m, 8H), 1.30 (m, 8H), 0.92 (dt, $J = 8.0$ Hz, 12H). ^{13}C NMR (100 MHz, D_2O , Me_4Si): δ 172.93, 153.24, 148.30, 137.95, 125.65, 123.63, 58.00, 23.08, 19.07, 12.77. Found: C, 39.0; H, 6.2; N, 5.1; V, 20.4. Number of peroxy-bonds: 0.25 per V atom.

V-OC@IL-1.5: ^1H NMR (400 MHz, D_2O , Me_4Si) δ 8.62-7.71 (m, 4H), 3.19 (m, 8H), 1.56 (m, 8H), 1.30 (m, 8H), 0.92 (dt, $J = 8.0$ Hz, 12H). ^{13}C NMR (100 MHz, D_2O , Me_4Si): δ 172.93, 153.24, 148.30, 137.95, 125.65, 123.63, 58.00, 23.08, 19.07, 12.77. Found: C, 52.8; H, 8.2; N, 5.7; V, 9.5. Number of peroxy-bonds: 0.44 per V atom.

V-OC@IL-2: ^1H NMR (400 MHz, D_2O , Me_4Si) δ 8.40-7.17 (m, 4H), 3.19 (m, 8H), 1.56 (m, 8H), 1.30 (m, 8H), 0.92 (dt, $J = 8.0$ Hz, 12H). ^{13}C NMR (100 MHz, D_2O , Me_4Si): δ 172.93, 153.24, 148.30, 137.95, 125.65, 123.63, 58.00, 23.08, 19.07, 12.77. Found: C, 55.4; H, 8.3; N, 6.2; V, 6.3. Number of peroxy-bonds: 0.55 per V atom.

Preparation of $\text{K}_2[\text{VO}(\text{O}_2)_2(\text{pic})]$

$\text{K}_2[\text{VO}(\text{O}_2)_2(\text{pic})]$ was prepared according to the method reported,²⁸ a clear pale green solution was obtained after heating a mixture of V_2O_5 (0.364g, 2.5 mmol) and KOH (0.494 g, 8.8 mmol) in H_2O (5.0 mL). 30% H_2O_2 (3.4 mL, 5.16 mmol) was added to this solution, upon which the solution became deep yellow with some effervescence. The mixture was stirred for 10 min and cooled at 5 °C in a water bath. A solution of 2-picolic acid (0.542 g, 4.4 mmol) in ethanol (7 mL) was then added, resulting in a color change to orange-red with the formation of some yellow precipitate. 2.0 mL of H_2O_2 was added to dissolve the precipitate and stand for 30 min. Then, 6.0 mL ethanol was added to the solution, which was then cooled at 5 °C for 3 days, where upon yellow crystals formed. They were collected by filtration, washed with cold ethanol, and dried overnight in vacuo. IR: $\nu(\text{CO})$ 1633 (s), 1590 (vs); $\nu(\text{VO})$ 948 (vs); $\nu(\text{OO})$ 867 (vs), 885 (m) cm^{-1} . Anal. Calc. for $\text{C}_6\text{H}_8\text{K}_2\text{NO}_9\text{V}$: C, 21.6; H, 1.2; N, 4.2. Found: C, 21.0; H, 1.3; N, 4.1.

Typical procedure for catalytic oxidation of alkanes

The alkane oxidations were typically carried out in air in thermostated (50 °C) Pyrex cylindrical vessels with vigorous stirring and using CH_3CN as solvent (up to 4.5 mL

total volume). Typically, the IL-stabilized V-OC@IL-1 (0.010g, 0.02 mmol V atom) was used as a catalyst, the alkane substrate, typically cyclohexane (0.42 g, 5.0 mmol) was then introduced, and the reaction started when hydrogen peroxide (30 % aqueous solution, 1.13g, 10 mmol) was added in one portion. The final concentrations of the reactants in the reaction mixture were as follows: catalyst V-OC@IL-1 ($0.0046 \text{ mol}\cdot\text{L}^{-1}$), substrate ($1.11 \text{ mol}\cdot\text{L}^{-1}$) and H_2O_2 ($2.22 \text{ mol}\cdot\text{L}^{-1}$). The reaction progress was monitored by chromatographic (GC), and the yield of products was determined by GC analysis using dodecane as the internal standard. After completion of the reaction, ethyl ether ($3 \text{ mL}\times 3$) was added for extraction. The upper organic phase was reduced by PPh_3 , and then used for GC analysis. Thereafter, the lower aqueous phase was evaporated to recover the catalyst. Quantitative determination of cyclohexane, cyclohexanol, cyclohexanone was carried out by GC using individual calibration curve method (Fig. S14-S16), and the correction factors were obtained accordingly. An example of chromatogram analysis of reaction solution was shown in Fig. S17. The products obtained are identified via the retention time and quantified via the calibration line as described above. The experimental data were repeated three times, and the standard deviations for conversion and yield are within $\pm 3\%$.

Reaction Kinetics

The procedure for investigating the kinetic parameters for the oxidation of cyclohexane was shown as follows. The concentration of catalyst was constant in all experiments (0.004 M). In order to examine the effect of substrate concentration on the rate of oxidation of cyclohexane, the concentration of cyclohexane was varied from 0.222 to 1.556 M, while the concentration of H_2O_2 was 2.22 M. Similarly, the effect of H_2O_2 concentration on the rate of oxidation of cyclohexane was investigated through adjusting the concentration of H_2O_2 from 0.556 to 2.22 M, while the concentration of cyclohexane was 1.11 M. The other reaction conditions have been given in the figure captions (Fig. S10 and S11). The reaction was monitored using GC. Oxygenate formation W_0 for the kinetic studies were determined from the slopes of reaction profiles (yield of KA oil vs time) at low yield (Conversion < 15%, initial rate method) according to Equation (1). The activation energy for the process was determined using the Arrhenius equation based on the calculated rate constants at different temperatures according to a previously reported method.^{29,30} The initial substrate concentration can be considered to be a constant during the oxidation reaction in a relatively large

concentration range, and thus the activation energy can be obtained by using the initial oxidation rate W_0 .

$$W_0 = (-d[\text{RH}]/dt) = d[\text{ROH} + \text{R}=\text{O}]/dt \quad (1)$$

where $[\text{RH}]$ denoted the concentration of cyclohexane while $[\text{ROH} + \text{R}=\text{O}]$ total concentration of cyclohexanol and cyclohexanone as determined by the reduction of the reaction mixture with PPh_3 .

Results and Discussion

Preparation and Characterization of V Oxo-cluster

The IL-stabilized vanadium oxo-clusters have been synthesized according to our previously reported procedure,²⁶ Briefly, the carboxylate IL $[\text{TBA}][\text{Pic}]$ was firstly synthesized by a careful neutralization of tetrabutylammonium hydroxide (TBAOH) and 2-picoline acid at room temperature. Thereafter, the vanadium oxo-clusters were synthesized by the reaction of vanadium peroxide species with the IL $[\text{TBA}][\text{Pic}]$ and designated as V-OC@IL- n , where n represented the molar ratio of the IL to V atoms.

The composition of the as-synthesized oxo-clusters was sequentially analyzed by elemental analysis, inductively coupled plasma atomic emission spectroscopy (ICP-AES), potential difference titration of $\text{Ce}^{3+}/\text{Ce}^{4+}$ and ^{51}V NMR. The number of peroxy-bond ranged from 0.25 to 0.55 per V atom in the vanadium oxo-clusters by potential difference titration of $\text{Ce}^{3+}/\text{Ce}^{4+}$, suggesting that a trace of peroxy-bonds in these vanadium oxo-clusters was still reserved (Table 1). In the light of these results, it is assumed the anion (picolinate) form a layer around the surface of vanadium oxo-cluster, leading to a center of negatively charge, and thus the cation of IL (TBA) existed at the outer layer for charge balance. In general, the IL plays a critical role in preventing the V species from generating the larger aggregates.

Table 1. Physicochemical data of the different vanadium oxo-clusters

Catalysts	Element analysis				Peroxy-bond/V	Color ^a	XRD
	C /%	H /%	N /%	V /%			
V-OC@IL-0.5	39.0	6.2	5.1	20.4	0.25	Brown	amorphous
V-OC@IL-1	46.9	7.1	5.9	10.6	0.35	Brown	amorphous
V-OC@IL-2	55.4	8.3	6.2	6.3	0.55	Red	amorphous

V_2O_5	-	-	-	-	-	Yellow	$\alpha-V_2O_5$
----------	---	---	---	---	---	--------	-----------------

View Article Online

DOI: 10.1039/DOCY01401J

^a All the vanadium oxo-clusters were brown or red viscous liquid while the commercial V_2O_5 was a yellow powder.

In the next step, a commercial vanadium pentoxide (V_2O_5) and the IL-stabilized vanadium oxo-clusters were characterized by using XRD. The IL-stabilized vanadium oxo-clusters (V-OC@IL-0.5, V-OC@IL-1, V-OC@IL-2) all showed amorphous structure (Fig. S1a-c). Comparatively, the commercial V_2O_5 showed clearly the characteristic peaks at 15.3° , 20.3° , 21.7° , 26.1° , 31.0° , 32.4° and 34.3° , assigning to (200), (001), (101), (110), (301) (011) and (310) planes of the $\alpha-V_2O_5$ structure, respectively (PDF # 41-1426, Fig. S1d).³¹ This result demonstrated clearly that the incorporation of the IL to peroxy-vanadate indeed changed the structure of the vanadium oxo-peroxo species, which were completely distinct from the commercial crystalline V_2O_5 . On the basis of the results above, the chemical properties of vanadium oxo-clusters, together with V_2O_5 was summarized in Table 1.

The thermal stability of the IL-stabilized vanadium oxo-clusters was then examined by TG analysis. As in Fig. S2, TGA curves displayed obvious weight losses of approximately 70.5%, 80.8% and 89.7% between 40 and 800 °C for the V-OC@IL-0.5, V-OC@IL-1 and V-OC@IL-2, respectively. The thermal degradation of the three oxo-clusters proceeded approximately with four main degradation steps. The pyrolysis processes correspond to the loss of peroxygen species (40–96°C); the detachment of adsorbed water molecules (96–180°C); the decomposition of tetrabutylammonium cations (180–400°C); and the degradation of picolinate ligands (400–550°C), respectively according to previous reports.^{26,32} After 550 °C, accompanying with the formation of vanadium oxide, the weight did not lose any more. The residual vanadium oxide contents closely corresponded to the results of ICP-AES analysis.

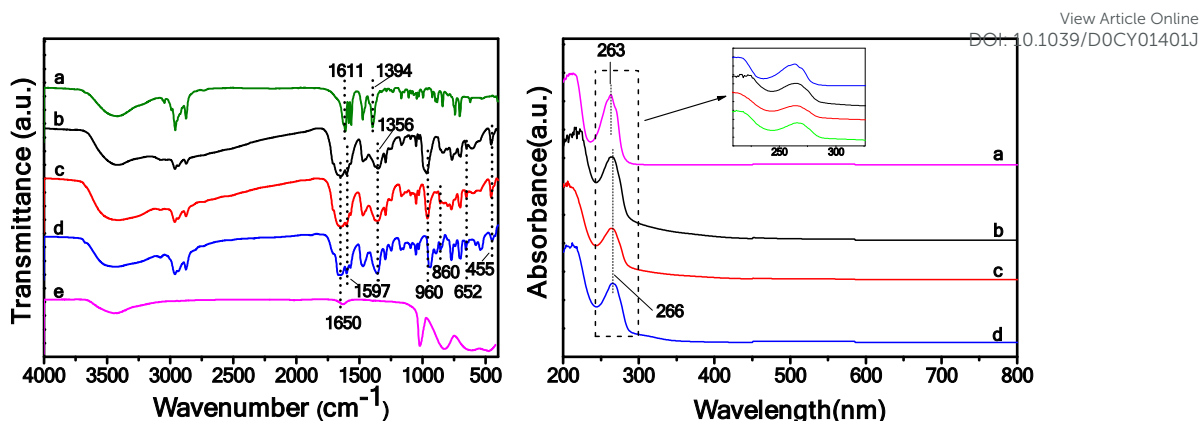


Figure 1. FT-IR spectra (left) and Uv-vis spectra (right) of the IL ([TBA][Pic]) and IL-stabilized vanadium oxo-clusters with different molar ratio of [TBA][Pic] to V. a) [TBA][Pic], b) V-OC@IL-0.5, c) V-OC@IL-1, d) V-OC@IL-2, e) V₂O₅.

Next, the three vanadium oxo-clusters were characterized by using FT-IR spectra, respectively. As shown in Fig. 1 (left), the band in sole IL [TBA][Pic] at 2869 and 2950 cm⁻¹ was related to $\nu(\text{C-H})$ and the band around 1300–1500 cm⁻¹ was characteristic for $\delta(\text{C-N})$, which all indicated the presence of the tetrabutylammonium cation. Besides, the bands at 650–1000 cm⁻¹ and 1100 cm⁻¹ were also attributed to the vibration of $\sigma(\text{C-H})$ and C–O bonds in the IL, respectively.³³ It was seen that the V₂O₅ displayed a broad band centered at *ca.* 1000cm⁻¹ and 640 cm⁻¹, which can be attributed to $\nu(\text{V=O})$ and $\nu_{\text{as}}(\text{V-O-V})$, respectively (Fig. 1e, left).^{32,34} For the IL-stabilized vanadium oxo-clusters, the bands at 1356 cm⁻¹ are due to the symmetric of carboxylate groups from picolinate (Fig. 1b–d, left),^{35–37} which were red-shifted, compared to that of carboxylate group in the sole IL [TBA][Pic] (1394 cm⁻¹) (Fig. 1a, left). Moreover, the bands assigning to $\nu(\text{C=N})$ at 1611 cm⁻¹ of [TBA][Pic] also red-shifted to 1597 cm⁻¹ in oxo-clusters.^{32,38} The changes of these peaks are caused by the coordination of picolinate with vanadium site. In addition, a wide band around 3420 cm⁻¹ was assigned to $\nu(\text{O-H})$ and a peak at *ca.* 1650 cm⁻¹ was related to the adsorbed water molecules in the oxo-clusters (Fig. 1b–d, left).³⁹ On the other hand, the large and sharp vibrational peak at approximately 960–970 cm⁻¹ belonged to $\nu(\text{V=O})$,³⁵ which was a red-shift compared to the commercial V₂O₅ owing to the influence of organic ligand. In the vanadium oxo-clusters, the new vibrational peaks around 652 cm⁻¹ were assigned to be $\nu_{\text{as}}(\text{V-O-V})$,³⁴ indicating that the polyoxovanadates existed as multinuclear vanadium instead of a mononuclear form. The new peaks at 455 cm⁻¹ of the oxo-clusters were characteristic for $\nu(\text{V-N})$ due to the coordination of the pyridine ring and the atom V.³² Furthermore,

the weak vibrational peak around 860 cm^{-1} arising from (O–O) species were also observed in the oxo-clusters. Especially, the peak of (O–O) strengthened gradually along with the increasing fraction of IL in the oxo-clusters, which revealed that the introduction of IL enables to stabilize the peroxy-bond ligand. This evidence was also in very well agreement with the potential difference titration analysis, which showed that the peroxy-bonds per V atom increased from 0.25 to 0.55 with IL dosages (Table 1).

Then, the vanadium oxo-clusters were subjected to Uv-vis characterization. As shown in Fig. 1 (right), the electronic bands of the free ligand (picolinate) and the vanadium oxo-clusters indicated a strong absorption band around 200–265 nm due to charge transfer within the ligand. The slight bathochronic shift of the band observed in these oxo-clusters caused by the interaction of the vanadium sites with the chromophores O=C=O and C=N, as compared with that of free [TBA][Pic].³⁸ The characterization of the FT-IR and the Uv-vis spectra strongly suggests that the coordination of vanadium sites with IL anion (picolinate) occur and the multinuclear vanadate species be formed.

EPR investigation was carried out to gain a deep insight into the feature of the valance state of vanadium species (Fig. S3).⁴⁰⁻⁴³ A typical of V(IV) $3d^1$ centers, with eight-line hyperfine patterns derived from the interaction of the free unpaired electron of V^{4+} and the nuclear magnetic moment of ^{51}V ($I = 7/2$) can be observed clearly. The tetravalent vanadium in V-OC@IL-0.5, V-OC@IL-1 and V-OC@IL-2 oxo-clusters accounted for 39%, 32% and 37% of the total vanadium according to the standard curve of EPR strength and vanadium (IV) concentration, respectively (Fig. S3b–d). This reflected that the vanadium species of the IL-stabilized oxo-clusters existed in the form of a mixed valence state.

Next, ^{51}V NMR spectra were used to examine the chemical environment of the V sites in the oxo-clusters.^{44,45} As shown in Fig. 2, the V-OC@IL-0.5 and V-OC@IL-1 showed three resonance signals, around -420 ppm , -500 ppm and -520 ppm , respectively, which were all corresponded to oligomeric vanadium sites.³⁰ Besides, ^{51}V NMR signal of two catalysts were very close to each other (Fig. 2a and 2b), indicating that coordination environment of V sites did not display obvious changes at low dosage of IL. However, V-OC@IL-1.5 displayed two resonance signals around -500 ppm and

–575 ppm (Fig. 2c), and these resonance signals were typical for oxo-vanadate oligomers, but the oligomeric state of vanadium might be different from that at lower IL dosages. As the IL dosages increased further, the resultant V-OC@IL-2 showed three resonance signals at –623 ppm, –652 ppm and –739 ppm, respectively (Fig. 2d). Comparatively, the chemical shifts of vanadium sites obviously moved to the higher field, and interestingly the signal at –739 ppm can be assigned to the mononuclear vanadium complex $[\text{VO}(\text{O}_2)_2(\text{pic})]^{2-}$.²⁸ Therefore, with increasing amount of IL, more picolinate could coordinate with vanadium sites, at least partial vanadium species in V-OC@IL-2 may exist in the mononuclear form. Based on ^{51}V NMR spectra studies, it indicated that the oligomeric states of vanadium in the oxo-clusters was strongly dependent on the molar ratio of IL to V. An increasing dosage of IL may tend to transform oligomeric vanadium species into mononuclear vanadium complexes.

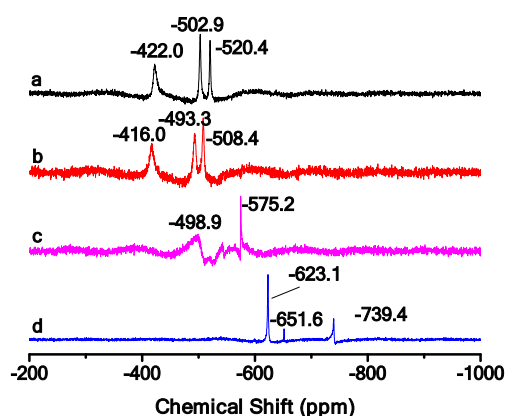


Figure 2. ^{51}V NMR spectra of the [TBA][Pic] stabilized vanadium oxo-clusters. a) V-OC@IL-0.5, b) V-OC@IL-1, c) V-OC@IL-1.5, d) V-OC@IL-2.

Although ^{51}V NMR spectra revealed that the IL-stabilized vanadium oxo-clusters (V-OC@IL- n , $n=1, 2$) might exist in the different forms, the corresponding oligomeric state was still unclear. To identify the possible structure forms of different vanadium species, the matrix assisted laser ionization time of flight mass spectrometry (MALDI-TOF) analysis in the negative mode was subsequently applied to determine the oligomeric structure of the vanadium oxo-clusters in water. As shown in Fig. S4a and S4b, the ion center of V-OC@IL-1 mainly appeared at 524.8 m/z , 540.8 m/z and 631.1 m/z , and the ion center of V-OC@IL-2 appeared at 343.0 m/z , 410.0 m/z , 441.9 m/z , 458.9 m/z , 631.1 m/z , the corresponding possible structures are shown in Table S1

(entries 1–7), which meant that the vanadium of oxo-cluster V-OC@IL-1 exist in the form of a trimer state rather than mononuclear state, while V-OC@IL-2 may exist in the form of a mix state of both mononuclear and oligomer state of vanadium.

View Article Online
DOI: 10.1039/D0CY01401J

Catalytic Activity

Cyclohexane oxidation was initially adapted as a model reaction to evaluate the catalytic performance. Firstly, the effects of the H₂O₂ amount and reaction temperature on cyclohexane oxidation were shown in Fig. S5 and Fig. S6, respectively. It was observed that two equivalents of H₂O₂ were enough for this reaction, more H₂O₂ had negative impact on catalytic efficiency (Fig. S5). This is probably due to the accumulation of water along with the consumption of more H₂O₂. Nevertheless, an increase of concentration of water would lower the oxidation rate in the reaction.³⁰ Besides, with a rise of reaction temperature, the oxidation activity increased and reached the maximum at 50 °C, but the activity dropped down along with further increase of temperature (Fig. S6). Obviously, the present reaction only occurred effectively under the appropriate temperature. Otherwise, an ineffective decomposition of H₂O₂ was not beneficial for the reaction.

The conversion/time profiles of cyclohexane oxidation over the different V-based catalysts with H₂O₂ as an oxidant were subsequently examined and then shown in Fig. 3. The mononuclear vanadium complex K₂[VO(O₂)₂(pic)] gave very poor activity. Commercial V₂O₅, afforded only 13% of total yield in 4.0 h. Notably, the IL-stabilized vanadium oxo-clusters exhibited much more higher catalytic activity even without adding any other additives under the identical conditions, indicating that the vanadium oxo-clusters are preferable to either mononuclear vanadium complex K₂[VO(O₂)₂(pic)] or commercial V₂O₅. In particular, the V-OC@IL-1 offered the highest catalytic activity (total yield of KA oil: about 30 %), and both the oxo-clusters V-OC@IL-0.5 and V-OC@IL-1 were much better than other catalysts and enable to complete the oxidation reaction within 1.0 h, after which the yield of KA oil basically increased no more. This feature was in accordance with the similar coordination structure of V sites between V-OC@IL-0.5 and V-OC@IL-1 catalysts, as reflected from the ⁵¹V NMR spectra (Fig. 2a vs 2b). In addition, as the IL/V molar ratio in the vanadium oxo-clusters was more than 1.5, the total yield of products (A and K) on V-OC@IL-1.5 and V-OC@IL-2 catalysts decreased to *ca.* 26 % and 18 %, respectively. These results demonstrated clearly that with the increase of IL dosages, vanadium aggregates

transformed gradually from trimer into binuclear and/or mononuclear, which caused a decrease of catalytic activity. In other words, the oligomeric vanadium species like trimer and dimer were much more active than that of the mononuclear vanadium species in the oxidation of cyclohexane.

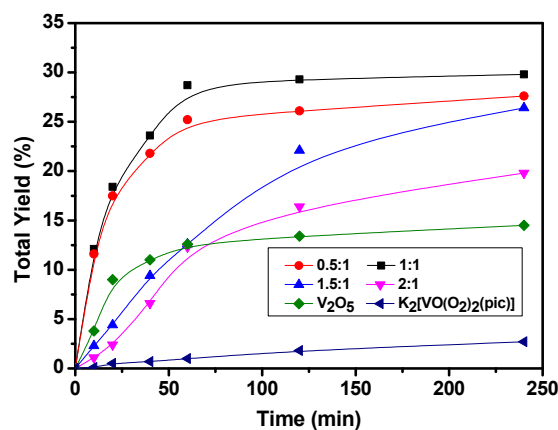


Figure 3. Total yield (KA oil) /time profiles of cyclohexane oxidation reactions over the different catalysts. Reaction conditions: cyclohexane (5.0 mmol), H₂O₂ (10.0 mmol, 30% aqueous solution), catalyst (0.4 mol%), CH₃CN (3.0 mL), 50 °C.

Interestingly, the initial reaction rate over V₂O₅ was faster than that on V-OC@IL-1.5 and V-OC@IL-2, but it levelled off after 60 min and the final yield of KA oil was only 13%, which was far lower than that of V-OC@IL-1.5 and V-OC@IL-2 (Fig. 3). To clarify the reason, the amount of residual H₂O₂ was determined by potential titration after reaction for 1.0 h. As shown in Table 2, either [TBA][Pic] or vanadium complex K₂[VO(O₂)₂(pic)] did not activate H₂O₂ and hardly consume H₂O₂ under the present conditions (Table 2, entries 2 and 3). The commercial V₂O₅ decomposed H₂O₂ very rapidly and thus gave low yield of products (Table 2, entry 4). In contrast, for the IL-stabilized V oxo-cluster catalysts, the decomposition of H₂O₂ was inhibited drastically and enhanced utilization efficiency of H₂O₂ via the coordination of picolinate anion (Table 2, entries 5–8). Moreover, the decomposition rates of H₂O₂ were also determined over commercial V₂O₅ and the V-OC@IL-1 catalysts for comparison. As shown in Fig. S7, even in the absence of substrates the V-OC@IL-1 was indeed capable to suppress the invalid decomposition of H₂O₂, compared to that of the commercial V₂O₅. This can be attributing to the coordination of IL anion with V sites, stabilizing oligomeric peroxovanadate species. It has been demonstrated that the coordination of the electron-

withdrawing ligand with metal sites played a crucial role in suppressing the decomposition of H₂O₂ due to higher the potential energy surface.⁴⁶

View Article Online
DOI:10.1039/C0CY01401J

Table 2. Oxidation of cyclohexane with the different catalysts^a

Entries	Catalysts	Yield/%			Residual H ₂ O ₂ /mmol
		A	K	Total	
1	blank	0	0	0	9.96
2	[TBA][Pic]	0	0	0	9.97
3	K ₂ [VO(O ₂) ₂ (pic)]	0.8	0.2	1.0	9.94
4	V ₂ O ₅	9.5	3.1	12.6	0.90
5	V-OC@IL-0.5	19.4	5.8	25.2	3.71
6	V-OC@IL-1	26.2	2.5	28.7	4.05
7	V-OC@IL-1.5	9.7	2.9	12.6	8.31
8	V-OC@IL-2	4.8	1.7	6.5	9.35
9 ^b	V ₂ O ₅	9.7	1.6	11.3	1.75
10 ^c	V ₂ O ₅	9.8	1.1	10.9	3.30
11 ^d	V ₂ O ₅	9.7	3.0	12.7	0.76

^a Reaction conditions: cyclohexane (5.0 mmol), H₂O₂ (10.0 mmol, 30% aqueous solution), catalyst (0.4 mol%), CH₃CN (3.0 mL), 50 °C, 1 h. The mass balance for the cyclohexane oxidation was normally higher than 98%. The standard deviations for product yield are within ±3%. ^{b,c,d} [TBA][OAc], [BMIM][OAc] and [BMIM][BF₄] were used as additive, respectively.

Structural Evolution of V oxo-cluster in the Presence of H₂O₂

⁵¹V NMR spectra have been proved a powerful tool to gain more insight of the possible evolution of active vanadium species in the process of the reaction.⁴⁷ Thus the oxidizing species of the different catalysts were characterized by ⁵¹V NMR spectra and shown in Fig. 4. Briefly, these catalysts (0.1 mmol) was first dissolved in mixture of H₂O₂ (1 mmol) and D₂O (0.5 mL), and then the samples were taken for the measurement of ⁵¹V NMR spectra, respectively. The V-OC@IL-1 in the presence of H₂O₂ displayed completely different resonance signals from that of the parent catalyst. The NMR signals of vanadium sites moved to a higher field due to the addition of H₂O₂

(Fig. 2b vs Fig. 4a). The original three peaks appropriately at -416.0 , -493.3 and -508.4 ppm have evolved into only two peaks appeared at -598.7 ppm and -665.1 ppm, assigned to oxo-vanadate oligomers,³⁰ which revealed that the original three types of vanadium species have been transformed into two types of oligomeric vanadium species. However, as the V_2O_5 was dissolved in the H_2O_2 (pH \sim 3–4), the resonance signal at -693.7 ppm appeared (Fig. 4b), which can be assigned to mononuclear $[VO(O_2)_2(H_2O)]^-$ anion.⁴⁸ Comparatively, the ^{51}V NMR signals of the oxidizing species of $K_2[VO(O_2)_2(pic)]$ shifted from the original -743 ppm to around -690 ppm and -730 ppm in the presence of H_2O_2 , respectively, which indicated that the mononuclear vanadium complex $[VO(O_2)_2(pic)]^{2-}$ (-743 ppm) has evolved into its oxidizing species (Fig. 4c).²⁸ Thus it can be seen that the oxidizing species of V-OC@IL-1 were completely different from that of V_2O_5 and $K_2[VO(O_2)_2(pic)]$, and the V-OC@IL-1 did not degraded into a mononuclear vanadium species even under the action of excess H_2O_2 .

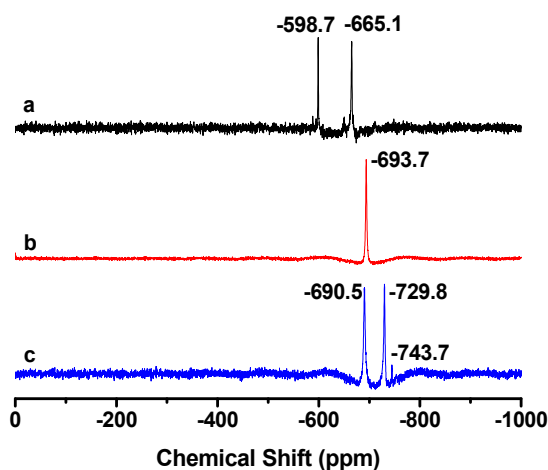


Figure 4. ^{51}V NMR spectra of oxidizing species of different catalysts in D_2O . a) V-OC@IL-1, b) V_2O_5 , c) $K_2[VO(O_2)_2(pic)]$.

FT-IR spectra and EPR spectra were also applied to investigate the changes of the V-OC@IL-1 under the action of H_2O_2 (Fig. S8). First, the oxo-cluster V-OC@IL-1 (0.2 mmol) was dissolved with 30% H_2O_2 (2.0 mmol). After the mixture was stirred for 10 min at 298 K, diethyl ether was rapidly poured into the solution to precipitate the

oxidizing species, followed by washing carefully with a small amount of diethyl ether. The resultant material was then characterized for the FT-IR (Fig. S8a). Compared with the fresh V-OC@IL-1, the peroxy-bond in the 860 cm^{-1} was significantly enhanced due to action of H_2O_2 . Besides, the vibrational peaks at 652 cm^{-1} assigned to $\nu_{\text{as}}(\text{V}-\text{O}-\text{V})$ still existed, suggested strongly that the V-OC@IL-1 did not dissociate completely into a mononuclear form after adding H_2O_2 , and more vanadium peroxy species were generated in the form of vanadium oligomeric state under the action of H_2O_2 . Meanwhile, the oxo-cluster V-OC@IL-1 (0.2 mmol) was dissolved with 30% H_2O_2 (2.0 mmol) and used for EPR test. Interestingly, no any EPR signals appeared (Fig. S8b), indicating the tetravalent vanadium species in the parent catalyst have been oxidized to pentavalent vanadium.

In order to identify the possible evolution structure of active species during the reaction, V-OC@IL-1 (0.02 mmol) was dissolved in 4 mL aqueous solution with 30% H_2O_2 (0.2 mmol) for mass spectra analysis to determine the structure change of the V-OC@IL-1 in the presence of H_2O_2 (Fig. S4c). The ion centered at 631.1 m/z still existed, meantime, new ion centered at 441.9 m/z and 458.9 m/z appeared, possible structures are listed in Table S1(entries 5–7), which meant that the vanadium of V-OC@IL-1 indeed existed in the form of trimer and dimer coordinated with picolinate, but was not dissociated into mononuclear vanadium under the action of H_2O_2 . Based on the characterization results above, it is demonstrated that trimer oxo-cluster V-OC@IL-1 could degrade partially into dimer but not into mononuclear vanadium under the action of excess H_2O_2 . Moreover, vanadium dimers and trimers existed in peroxy form are the actual active species for the cyclohexane oxidation reaction, the result is consistent with the literature report, dinuclear peroxidovanadates are believed to play an important role in vanadium-catalyzed oxidations.^{30,45,49}

Role of specific IL in Forming Oligomeric Vanadium Species

The IL is an interesting medium for the formation and stabilization of catalytically active metal or metal oxoclusters.^{50–52} The pre-organized supermolecular structures of ILs can create an external layer around the nanostructure to control the growth of nano-aggregates and affect the mass transportation.^{53,54} It indicated the size of the aggregates is strongly dependent on the degree of internal structure of the IL. However, simple ionic liquids could not provide an effective protection to the nanoparticles against aggregation. As shown in Fig. 4b, the mononuclear $[\text{VO}(\text{O}_2)_2(\text{H}_2\text{O})]^-$ anion was

observed via reaction of the sole V_2O_5 and H_2O_2 under room temperature conditions, in line with the previous report.⁴⁸ Sequentially, the common ILs have been used to confirm if they can induce V_2O_5 to form oligomeric vanadium species. Firstly, V_2O_5 was dissolved under the action of excess H_2O_2 and then mixed with three common ILs ([TBA][OAc], [BMIM][OAc] and [BMIM][BF₄]), respectively (the molar ratio of IL/V=1:1). The ⁵¹V NMR spectra of the solution were shown in Fig. S9. The results showed that the chemical shifts of vanadium species in the presence of the three general ILs showed no obvious change compared to that of the sole V_2O_5 in H_2O_2 (Fig. 4b), indicating that these ILs did not interact with vanadium sites. The vanadium species still existed as mononuclear $[VO(O_2)_2(H_2O)]^-$ anion. In addition, the as-synthesized vanadium catalysts by using the three different ILs showed almost the same yield of KA oil in cyclohexane oxidation as that of the sole V_2O_5 -based catalyst (Table 2, entries 4 vs 9–11), which is consistent with the results of ⁵¹V NMR spectra. As such, the common ILs cannot induce to generate the catalytically active oligomeric vanadium species from V_2O_5 precursor.

To identify the crucial role of the IL [TBA][Pic], further investigation is needed to clarify whether the dimeric or trimeric assembly of oligomeric vanadium(V)-peroxo species were formed due to the addition of [TBA][Pic]. It indicated that once IL [TBA][Pic] was introduced into the above solution under the similar conditions, MS confirmed that the dimeric or trimeric assembly of vanadium(V)-picolinate-peroxo species appeared in the solution. As shown in Fig. S4d, the ions centered at 458.9 m/z and 631.6 m/z assigning to dimeric or trimeric vanadium species were consistent with that of oxidizing species of V-OC@IL-1 (Fig. S4c). Besides, if the fresh solution above was employed for cyclohexane oxidation, the total yield of A and K (around 27.8%) was almost identical to that of V-OC@IL-1 (around 28.7%). The results indicated unambiguously that the addition of IL [TBA][Pic] induced to form dimer and trimer from mononuclear $[VO(O_2)_2(H_2O)]^-$ complexes rather than to form the other mononuclear vanadium complexes. The role of the present IL enabled the vanadium species to maintain the appropriate oligomer states without further aggregation. This may be related to the specific dimensions of the domains of IL itself,^{53,55} along with the coordination of anion, which leads to generate oligomeric vanadium(V)-picolinate-peroxo species.

Kinetic Studies and Reaction Mechanism

The kinetics of cyclohexane oxidation over V-OC@IL-1 catalyst has been investigated thoroughly. Prior to kinetic studies, the effects of stirring speed and catalyst amount on the reaction rate have been screened to exclude the diffusion restrictions. Stirring speed could be set to be more than 800 rpm, and the concentration of vanadium catalyst was kept constant (0.004 M) for the kinetics study. Dependence of the initial rate of oxygenate formation W_0 on initial concentration of cyclohexane ($[\text{cyclohexane}]_0$) and H_2O_2 ($[\text{H}_2\text{O}_2]_0$) were shown in Fig. S10 and Fig. S11, which demonstrated the linearization of W_0 and $[\text{cyclohexane}]_0$ or $[\text{H}_2\text{O}_2]_0$ as their initial concentrations were in a certain range, respectively (Inset). The W_0 was derived from the initial rate of oxygenate formation, which was highly dependent on either the initial concentration of cyclohexane or H_2O_2 (Fig. S10 and Fig. S11). These results implied that the rate-limiting transition state could not only be involved in the conversion of cyclohexane, but also in the activation progress of H_2O_2 , which is consistent with the previous report.¹⁶ Additionally, the dependence of the initial rate of oxygenate formation W_0 on the temperature (Arrhenius plots, 303–323 K) was shown in Fig. 5. The linearity of the Arrhenius plots was examined to determine the activation energy, which was $E_a = 24.4 \text{ kJ mol}^{-1}$. The activation energy obtained is indeed similar to the previous report on oligomeric vanadium-catalyzed cyclohexane oxidation.³⁰

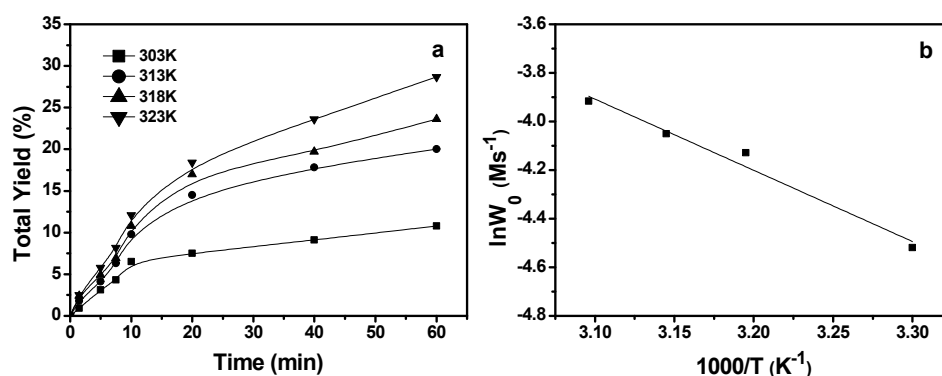


Figure 5. a) Total yield (KA oil)/time profiles of cyclohexane oxidation reactions catalyzed by V-OC@IL-1 at different temperatures. b) Arrhenius plots for the oxidation reaction of cyclohexane and H_2O_2 . The observed oxygenate formation W_0 were calculated with the initial rates at different temperatures. Reaction conditions: cyclohexane (1.11 M), H_2O_2 (2.22 M, 30% aqueous solution), V-OC@IL-1 (0.004 M), CH_3CN (3.0 mL).

It was indicated that the cyclohexane oxidation was initiated by free radicals on

vanadium-based catalysts in the presence of H_2O_2 . Next, it was important to understand whether the reaction is a free radical-initiated reaction. As shown in Fig. S12, if the free radical annihilator 2,6-di-tert-butyl-4-methylphenol (BHT) was added at the beginning of reaction, the yield to KA oil dropped down sharply, and even the reaction almost did not occur in the presence of 3 mmol of BHT. Therefore, the catalytic oxidation of cyclohexane by vanadium oxo-cluster V-OC@IL-1 was most possibly involved a free radical reaction mechanism.

Some chemical and biochemical systems involving vanadium are also known to generate hydroxyl radicals.⁵⁶⁻⁵⁸ The spin trap method is widely used for the fixation of radicals that arise in various chemical and biochemical reactions.⁵⁹ In order to identify the possible presence of hydroxyl radicals and their participation in hydrocarbon oxidations by the V-OC@IL-1, the interaction of nitron with a hydroxyl radical gives rise to the formation of the radical adduct. As shown in Fig. 6, a solution containing V-OC@IL-1 (0.004 M), cyclohexane (0.46 M) and the nitron (0.05 M) in acetonitrile after the addition of a 30% aqueous solution of hydrogen peroxide (final concentration was 0.1 M) exhibited a signal having a triplet structure with $g = 2.0057 \pm 0.0002$, $a_{\text{N}} = 13.75$ mT and $a_{\text{H}}^{\beta} = 2.25$ mT in the EPR spectrum. These parameters of the EPR spectrum agree well with the corresponding values for the adduct of nitron with hydroxyl radicals generated in the photolysis of hydrogen peroxide in acetonitrile ($g = 2.0054 \pm 0.0002$, $a_{\text{N}} = 15.5$ mT and $a_{\text{H}}^{\beta} = 2.35$ mT).²⁹ Thus, in the light of the results of free radical annihilator and EPR, it drew a conclusion that V-OC@IL-1 operates likely via a mechanism involving in $\text{HO}\cdot$ radical species. The present reaction mechanism is based on the generation of the $\text{HO}\cdot$ radicals by formation of H_2O_2 adduct with vanadium complex, and then the $\text{HO}\cdot$ radicals react with alkanes to form the oxidation products.^{16,17,56}

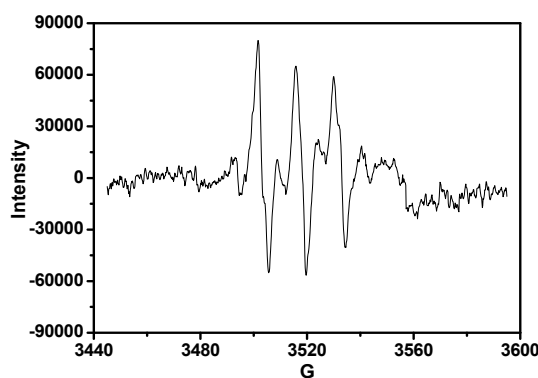


Figure 6. EPR Spectrum of a solution containing N-benzylidene-2-methylpropan-2-amine oxide. Reaction condition: V-OC@IL-1 (0.004M), cyclohexane (0.46 M) and the nitron (0.05 M) in acetonitrile after the addition of a 30% aqueous solution of hydrogen peroxide (0.1 M), 50 °C, 20 min.

Recyclability of the catalyst and Substrate scope

The present vanadium oxo-cluster catalysts have some advantages over the vanadium-based homogeneous catalysts reported in the previous literature.⁶⁰ They not only afforded high activity in the oxidation of cyclohexane, but also showed good recyclability. As shown in Fig. 7, after five recycles, the catalytic activity of oxo-cluster V-OC@IL-1 decreased slightly. The ICP-AES analysis indicated that trace of V leaching (26 ppm after 5 cycles) accounted for the decrease of activity rather than the structure of the catalyst had been changed, as confirmed by the EPR spectrum and ⁵¹V NMR spectrum of the recovered catalyst (Fig. S13). EPR spectrum of the spent catalyst displayed the almost same contents of tetravalent vanadium (35 % of total vanadium) with that of the fresh catalyst (32 % of total vanadium) (Fig. S13a vs S3c), and meantime the chemical shift of vanadium was basically the same as that of fresh catalyst (Fig. S13b vs Fig. 2b). These results demonstrated that the catalyst could be regenerated to its original state in the course of the catalytic cycles. Notably, the IL endowed the vanadium oxo-cluster catalysts with the good recyclability owing to the particular properties like such as nonvolatility, immiscibility with weak polar solvent and high thermal stability etc.

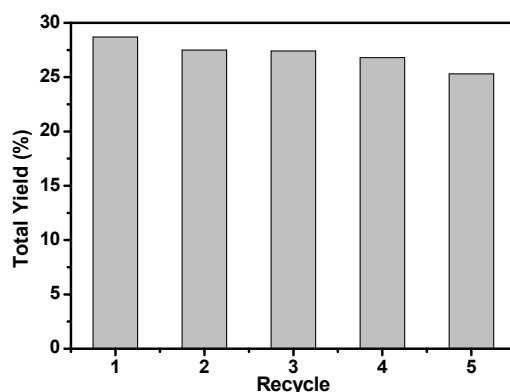


Figure 7. Catalytic recyclability over V-OC@IL-1 for the oxidation of cyclohexane. Reaction conditions: cyclohexane (5.0 mmol), H₂O₂ (10.0 mmol, 30% aqueous solution), catalyst (0.4 mol%), CH₃CN (3.0 mL), 50 °C, 1 h.

The present vanadium oxo-cluster catalyst was not only employed for the oxidation of sp^3 hybrid C–H bond, but also can be extended to the oxidation of aromatic C–H bonds without any other additives. For examples, a series of hydrocarbons were tested for oxidation to examine the substrate scope over the present vanadium oxo-cluster catalyst V-OC@IL-1. As shown in Table 3, the vanadium oxo-cluster catalyst was active against both cycloalkanes and bridged alkanes (Table 3, entries 1–4). Notably, in addition to sp^3 hybrid C–H bonds, the V-OC@IL-1 catalyst also exhibited a certain catalytic oxidation for sp^2 hybrid C–H bonds of aromatic compounds (Table 3, entries 5–8). In addition, due to the σ - π hyperconjugation between the α -position C–H bond of benzene ring and the π system of benzene, the bond energy of the C–H of the α -position decreased and the activity of α -H increased, which could lead to the product arisen from not only the hydroxylation of aromatic ring, but also the oxidation C–H bonds on the substituted alkyl group. Moreover, the aromatic ring with a strong electron-withdrawing group like nitrobenzene is inactive (Table 3, entry 9), less than benzene without any substituent (Table 3, entry 8), while the conversion of benzene homologs with electron-donating group afforded better results (Table 3, entries 5–7). Especially, ethylbenzene conversion can reach up to 21.5 % due to the electron-rich ethyl group. It was worth noting that the selectivity to oxidation of benzylic C–H bond accounted for 72.8%, which indicated that hydroxyl radical was the main oxidation species, because the presence of free HO· in the oxidation mainly led to the preferential activation of the benzylic C–H bond.⁶¹ Moreover, owing to the electron donating ability of methyl and methoxy is less than that of ethyl group, the reactivity of toluene and anisole were less than that of ethylbenzene correspondingly.

Table 3. Oxidation of different substrates with V-OC@IL-1

Entries	Substrates	Con./%	Products (Sel./%)
1 ^a	cyclohexane	30.3	cyclohexanol (86.5), cyclohexanone (13.5)
2 ^a	cyclooctane	19.6	cyclooctanol (58.9), cyclooctanone (41.1)
3 ^b	norbornane	6.1	2-norbornyl alcohol (80.6), 2-norbornone (19.4)
4 ^b	adamantane	6.0	1-adamantanol (56.8), 2-adamantanone (43.2)
5 ^c	ethylbenzene	21.5	benzaldehyde (5.2), 1-phenylethanol (13.0),

			acetophenone (54.6), 2-ethylphenol (3.3), 3-ethylphenol (10.4), 4-ethylphenol (13.5)
6 ^c	toluene	10.7	benzaldehyde (33.7), 2-methylphenol (31.7), 3-methylphenol (15.0), 4-methylphenol (19.6)
7 ^a	anisole	10.8	benzyl formate (30.5), 2-methoxyphenol (69.5)
8 ^b	benzene	6.5	phenol (99.9)
9 ^b	nitrobenzene	-	-

Reaction condition: Substrate (2 mmol), H₂O₂ (4 mmol), V-OC@IL-1 (0.4 mol%), CH₃CN (3.0 mL). ^a 50 °C, 4 h; ^b 40 °C, 12 h; ^c 30 °C, 12 h.

Finally, the catalytic performance of the present system was compared with that of the industrial process, as well as the other reported systems in the oxidation of cyclohexane to KA oil. As shown in Table S2, the yield of KA oil is much higher more when hydrogen peroxide is used as oxidant instead of oxygen. Besides, the catalytic performance of the current V-OC@IL-1 is comparable or even better than some other reported catalytic systems using hydrogen peroxide as oxidant. The present catalytic system exhibited the advantages of the shorter reaction time, higher utilization efficiency of hydrogen peroxide and no additional co-catalyst such as pyridine needed for the reaction. Especially, the present catalytic system can be recycled and also applied to the selective oxidation of other alkanes and aromatic hydrocarbons. For building a more efficient C–H bond oxidation catalysis, precise design to control the oligomeric states of the vanadium species would be highly promising and is currently underway in our laboratory.

Conclusion

This work demonstrated that the vanadium oxo-cluster has been developed by the condensation of peroxo vanadium species in the presence of the functionalized ionic liquid [TBA][Pic]. The picolinate anion in the IL acted as a ligand to stabilize the oligomeric vanadium oxo-cluster by coordination with the vanadium sites, while the cation of IL played the role in balancing charge and tuned the miscibility of vanadium oxo-cluster in solvents. The as-synthesized vanadium oxo-clusters were highly efficient for the catalyzing oxidation of cyclohexane with H₂O₂ as an oxidant. Especially, the oxo-cluster V-OC@IL-1 obtained approximately 30% total yield of KA oil without adding any co-catalyst at 50 °C in one hour, which is preferable to commercial V₂O₅

and mononuclear vanadium complex ($K_2[VO(O_2)_2(pic)]$). Furthermore, the structure of the V oxo-cluster almost reserved and the loss of activity was not obvious even after five cycles due to a negligible leaching of vanadium species. Notably, the oligmeric vanadium species are highly dependent on the molar ratio of IL to V atoms, and especially an excess of IL dosages would lead to producing inactive mononuclear vanadium species. The fresh V-OC@IL-1 existed as a main trimer vanadium species, and it was not degraded into mononuclear vanadium even under the action of excess H_2O_2 according to the characterization of ^{51}V NMR and MS spectra. Moreover, the present V oxo-cluster catalyst was extended for the activation of the sp^3 hybridized C–H and aromatic sp^2 hybridized C–H bond. EPR characterization demonstrated the V-OC@IL-1 operated via a mechanism of the $HO\cdot$ radical. This work is the first example of IL-stabilizing vanadium oxo-clusters owing high catalytic activity for the oxidation of inert C–H bonds. Undoubtedly, the design and construction of the novel oxo-cluster will open new avenues for achieving redox-active and stable catalysts.

Acknowledgements

The authors are grateful for support from the National Natural Science Foundation of China (21773061, 21978095), the innovation Program of Shanghai Municipal Education Commission (15ZZ031). Y. F. acknowledges the support by Ministry of Science and Technology of the People's Republic of China (Grant No. 2018YFC1602804 , 2018YFF01012504) and Microscale Magnetic Resonance Platform of ECNU.

References

- 1 N. Tsunoji, H. Nishida, Y. Ide, K. Komaguchi, S. Hayakawa, Y. Yagenji, M. Sadakane and T. Sano, *ACS Catal.*, 2019, **9**, 5742–5751.
- 2 M. Guo, M. S. Seo, Y. M. Lee, S. Fukuzumi and W. Nam, *J. Am. Chem. Soc.*, 2019, **141**, 12187–12191.
- 3 S. T. Wu, Y. R. He, C. H. Wang, C. M. Zhu, J. Shi, Z. Y. Chen, Y. Wan, F. Hao, W. Xiong, P. L. Liu and H. A. Luo, *ACS Appl. Mater. Interfaces*, 2020, **12**, 26733–26745.
- 4 W. B. Ma, Y. X. Qiao, N. Theyssen, Q. Q. Zhou, D. F. Li, B. J. Ding, D. Q. Wang and Z. S. Hou, *Catal. Sci. Technol.*, 2019, **9**, 1621–1630.

- 5 X. Liu, M. Conte, Q. He, D. W. Knight, D. M. Murphy, S. H. Taylor, K. Whiston, C. J. Kiely and G. J. Hutchings, *Chem. - Eur. J.*, 2017, **23**, 11834–11842. View Article Online
DOI: 10.1039/C6CY01401J
- 6 T. A. Fernandes, C. I. M. Santos, V. André, S. S. P. Dias, M. V. Kirillova and A. M. Kirillov, *Catal. Sci. Technol.*, 2016, **6**, 4584–4593.
- 7 X. Lyu, H. Mao, K. Zhu, Y. Kong and M. Kobayashi, *Microporous Mesoporous Mater.*, 2017, **252**, 1–9.
- 8 D. S. Nesterov, O. V. Nesterova and A. J. L. Pombeiro, *Coordin. Chem. Rev.*, 2018, **355**, 199–222.
- 9 D. Dragancea, N. Talmaci, S. Shova, G. Novitchi, D. Darvasiová, P. Rapta, M. Breza, M. Galanski, J. Kozišek, N. M. R. Martins, L. M. D. R. S. Martins, A. J. L. Pombeiro and V. B. Arion, *Inorg. Chem.*, 2016, **55**, 9187–9203.
- 10 E. P. Talsi and K. P. Bryliakov, *Coordin. Chem. Rev.*, 2012, **256**, 1418–1434.
- 11 Y. J. Zhang, Z. Yin, H. S. Hui, H. Wang, Y. P. Li, G. H. Liu, J. L. Kang, Z. H. Li, B. B. Mamba and J. X. Li, *J. Catal.*, 2020, **387**, 154–162.
- 12 M. Sutradhar, M. V. Kirillova, M. F. C. Guedes da Silva, L. M. D. R. S. Martins and A. J. L. Pombeiro, *Inorg. Chem.*, 2012, **51**, 11229–11231.
- 13 S. Gupta, M. V. Kirillova, M. F. C. Guedes da Silva, A. J. L. Pombeiro and A. M. Kirillov, *Inorg. Chem.*, 2013, **52**, 8601–8611.
- 14 P. Selvam and S. E. Dapurkar, *J. Catal.*, 2005, **229**, 64–71.
- 15 L. L. Bai, K. X. Li, Y. B. Yan, X. L. Jia, J. M. Lee and Y. H. Yang, *ACS Sustainable Chem. Eng.*, 2015, **4**, 437–444.
- 16 G. B. Shul'pin, *Catalysts*, 2016, **6**, 50–90.
- 17 R. R. Langeslay, D. M. Kaphan, C. L. Marshall, P. C. Stair, A. P. Sattelberger and M. Delferro, *Chem. Rev.*, 2019, **119**, 2128–2191.
- 18 C. N. Dai, J. Zhang, C. P. Huang and Z. G. Lei, *Chem. Rev.*, 2017, **117**, 6929–6983.
- 19 Y. X. Qiao, W. B. Ma, N. Theyssen, C. Chen and Z. S. Hou, *Chem. Rev.*, 2017, **117**, 6881–6928.
- 20 J. P. Hallett and T. Welton, *Chem. Rev.*, 2011, **111**, 3508–3576.
- 21 K. L. Luska, P. Migowski and W. Leitner, *Green Chem.*, 2015, **17**, 3195–3206.
- 22 W. W. Zhu, H. M. Yang, Y. Y. Yu, L. Hua, H. Li, B. Feng and Z. S. Hou, *Phys. Chem. Chem. Phys.*, 2011, **13**, 13492–13500.
- 23 W. W. Zhu, Y. Y. Yu, H. M. Yang, L. Hua, Y. X. Qiao, X. G. Zhao and Z. S. Hou, *Chem. - Eur. J.*, 2013, **19**, 2059–2066.
- 24 H. K. Stassen, R. Ludwig, A. Wulf and J. Dupont, *Chem. - Eur. J.*, 2015, **21**, 8324–

8335.

View Article Online
DOI: 10.1039/DOCY01401J

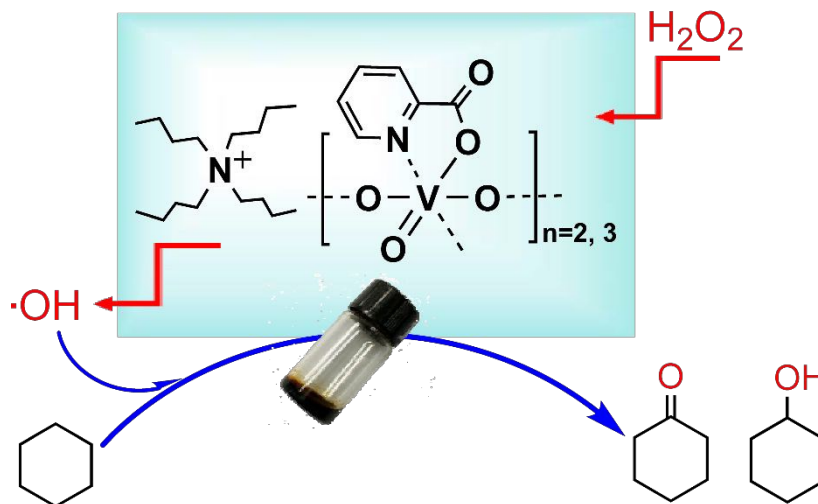
- 25 C. W. Scheeren, G. Machado, S. R. Teixeira, J. Morais, J. B. Domingos and J. Dupont, *J. Phys. Chem. B*, 2006, **110**, 13011–13020.
- 26 Q. Q. Zhou, M. Ye, W. B. Ma, D. F. Li, B. J. Ding, M. Y. Chen, Y. F. Yao, X. Q. Gong and Z. S. Hou, *Chem. - Eur. J.*, 2019, **25**, 4206–4217.
- 27 D. M. Wolfe and P. R. Schreiner, *Eur. J. Org. Chem.*, 2007, **17**, 2825–2838.
- 28 A. Shaver, J. B. Ng, D. A. Hall, B. S. Lum and B. I. Posner, *Inorg. Chem.*, 1993, **32**, 3109–3113.
- 29 G. B. Shul'pin, Y. N. Kozlov, G. V. Nizova, G. Süss-Fink, S. Stanislas, A. Kitaygorodskiy and V. S. Kulikova, *J. Chem. Soc., Perkin Trans.*, 2001, **2**, 1351–1371.
- 30 M. V. Kirillova, M. L. Kuznetsov, Y. N. Kozlov, L. S. Shul'pina, A. Kitaygorodskiy, A. J. L. Pombeiro and G. B. Shul'pin, *ACS Catal.*, 2011, **1**, 1511–1520.
- 31 Y. Chen, K. Muthukumar, L. Leban and J. Li, *Electrochim. Acta*, 2020, **330**, 135200–135208.
- 32 A. S. Barakat, A. S. Gaballa, S. F. Mohammed and S. M. Teleb, *Spectrochim. Acta. A*, 2005, **62**, 814–818.
- 33 C. Petibois and G. De'le'ris, *Analyst*, 2004, **129**, 912–916.
- 34 P. Román, A. S. José, A. Luque and J. M. Gutiérrez-Zorrilla, *Inorg. Chem.*, 1993, **32**, 775–776.
- 35 M. Mad'arová, M. Sivák, L. Kuchta, J. Marek and J. Benko, *Dalton Trans.*, 2004, **20**, 3313–3320.
- 36 J. Qiu, B. Vlasisavljevich, L. Jouffret, K. Nguyen, J. E. S. Szymanowski, L. Gagliardi and P. C. Burns, *Inorg. Chem.*, 2015, **54**, 4445–4455.
- 37 D. Bayot, B. Tinant and M. Devillers, *Inorg. Chem.*, 2004, **43**, 5999–6005.
- 38 C. L. Orjiekwe, F. A. S. Fabiyi and D. A. O. Edward, *Synth. React. Inorg. Met.-Org. Chem.*, 2005, **35**, 695–702.
- 39 A. Esteves, L. C. A. Oliveira, T. C. Ramalho, M. Goncalves, A. S. Anastacio and H. W. P. Carvalho, *Catal. Commun.*, 2008, **10**, 330–332.
- 40 T. Ben Zid, I. Khedher, Z. Ksibi and J. M. Fraile, *J. Porous Mater.*, 2016, **23**, 507–516.
- 41 H. Hu, F. Yang, R. H. Zhang, Y. H. Zhang, D. Y. Liu and G. M. Yang, *J. Mol. Struct.*, 2013, **1036**, 402–406.

- 42 F. Z. Ren, H. Y. Li, Y. X. Wang and J. J. Yang, *Appl. Catal., B*, 2015, **176–177**, 160–172. View Article Online
DOI: 10.1039/C5CY01401J
- 43 E. S. Bazhina, G. G. Aleksandrov, M. A. Kiskin, N. N. Efimov, E. A. Ugolkova, V. V. Minin, A. A. Sidorov, V. M. Novotortsev and I. L. Eremenko, *Russ. Chem. Bull., Int. Ed.*, 2014, **63**, 1475–1486.
- 44 D. Rehder, *Coordin. Chem. Rev.*, 2008, **252**, 2209–2223.
- 45 L. Krivosudský, P. Schwendt and R. Gyepes, *Inorg. Chem.*, 2015, **54**, 6306–6311.
- 46 W. B. Ma, H. Y. Yuan, H. F. Wang, Q. Q. Zhou, K. Kong, D. F. Li, Y. F. Yao and Z. S. Hou, *ACS Catal.*, 2018, **8**, 4645–4659.
- 47 N. R. Jaegers, C. Wan, M. Y. Hu, M. Vasiliu, D. A. Dixon, E. Walter, I. E. Wachs, Y. Wang and J. Z. Hu, *J. Phys. Chem. C*, 2017, **121**, 6246–6254.
- 48 N. J. Campbell, A. C. Dengel and W. P. Griffith, *Polyhedron*, 1989, **8**, 1379–1386.
- 49 A. S. Tracey, G. R. Willsky and E. S. Takeuchi, *Vanadium. Chemistry, Biochemistry, Pharmacology, and Practical Applications*, CRC Press, Taylor & Francis Group: Boca Raton, FL, 2007.
- 50 P. Priyananda, H. Sabouri, N. Jain and B. S. Hawkett, *Langmuir*, 2018, **34**, 3068–3075.
- 51 M. Qu, S. Chen, W. B. Ma, J. G. Chen, K. Kong, F. F. Zhang, H. Li, Z. S. Hou and X. M. Zhang, *Langmuir*, 2016, **32**, 13746–13751.
- 52 K. Shen, Z. H. Huang, J. H. Yang, G. Z. Yang, W. C. Shen and F. Y. Kang, *Carbon*, 2013, **58**, 238–251.
- 53 R. Hayes, G. G. Warr and R. Atkin, *Chem. Rev.*, 2015, **115**, 6357–6426.
- 54 V. S. Souza, J. D. Scholten, D. E. Weibel, D. Eberhardt, D. L. Baptista, S. R. Teixeira and J. Dupont, *J. Mater. Chem. A*, 2016, **4**, 7469–7475.
- 55 K. Dong, X. M. Liu, H. F. Dong, X. P. Zhang and S. J. Zhang, *Chem. Rev.*, 2017, **117**, 6636–6695.
- 56 M. Sutradhar, L. M. D. R. S. Martins, T. R. Barman, M. L. Kuznetsov, M. F. C. Guedes da Silva and A. J. L. Pombeiro, *New J. Chem.*, 2019, **43**, 17557–17570.
- 57 A. A. Alshaheri, M. I. M. Tahir, M. B. A. Rahman, T. B. S. A. Ravoof and T. A. Saleh, *Chem. Eng. J.*, 2017, **327**, 423–430.
- 58 R. Z. Khaliullin, A. T. Bell and M. Head-Gordon, *J. Phys. Chem. B*, 2005, **109**, 17984–17992.
- 59 C. Xu, L. L. Jin, X. Z. Wang, Y. Q. Chen and L. Y. Dai, *Carbon*, 2020, **160**, 287–297.

- 60 J. A. L. da Silva, J. J. R. Fraústo da Silva and A. J. L. Pombeiro, *Coordin. Chem. Rev.*, 2011, **255**, 2232–2248. [View Article Online](#)
DOI: 10.1039/D0CY01401J
- 61 Q. Y. Liu, L. F. Zhu, L. Li, B. Guo, X. K. Hu and C. W. Hu, *J. Mol. Catal. A: Chem.*, 2010, **331**, 71–77.

Table of contents

Ionic liquid-stabilizing V oxo-clusters



The specific ionic liquid ([TBA][Pic])-stabilizing the vanadium oxo-clusters exist in the form of trimer and dimer and were highly active for catalyzing C–H bond oxidation with H₂O₂ as an oxidant.